MOLECULAR AND CELLULAR BIOLOGY, Sept. 1993, p. 5479–5489
0270-7306/93/095479-11$02.00/0
Copyright © 1993, American Society for Microbiology
Vol. 13, No. 9

Selective DNA Bending by a Variety of bZIP Proteins

TOM K. KERPPOLA* AND TOM CURRAN
Roche Institute of Molecular Biology, Nutley, New Jersey 07110

Received 1 April 1993/Returned for modification 5 May 1993/Accepted 9 June 1993

We have investigated DNA bending by bZIP family proteins that can bind to the AP-1 site. DNA bending is widespread, although not universal, among members of this family. Different bZIP protein dimers induced distinct DNA bends. The DNA bend angles ranged from virtually 0 to greater than 40° as measured by phasing analysis and were oriented toward both the major and the minor grooves at the center of the AP-1 site. The DNA bends induced by the various heterodimeric complexes suggested that each component of the complex induced an independent DNA bend as previously shown for Fos and Jun. The Fos-related proteins Fra1 and Fra2 bent DNA in the same orientation as Fos but induced smaller DNA bend angles. ATF2 also bent DNA toward the minor groove in heterodimers formed with Fos, Fra2, and Jun. CREB and ATF1, which favor binding to the CRE site, did not induce significant DNA bending. Zta, which is a divergent member of the bZIP family, bent DNA toward the major groove. A variety of DNA structures can therefore be induced at the AP-1 site through combinatorial interactions between different bZIP family proteins. This diversity of DNA structures may contribute to regulatory specificity among the plethora of proteins that can bind to the AP-1 site.

The AP-1 site is a common regulatory element found upstream of many cellular and viral genes. This sequence element can mediate transcriptional responses to a variety of extracellular stimuli. Yet, despite the ubiquitous nature of the AP-1 binding site, many genes containing AP-1 sites are transcribed only in specific cell types or at specific developmental stages. This regulatory specificity may be generated through multiple interrelated mechanisms. Different AP-1 binding proteins may differ in their DNA-binding specificities, transcriptional activities, interactions with other transcription factors, and other properties that may contribute to their regulatory functions.

The AP-1 site and closely related sequence elements are recognized by dimeric complexes of bZIP family proteins including Fos-, Jun-, ATF-, and CREB-related proteins. The large number of possible homo- and heterodimeric combinations among these proteins provides an abundance of dimers that can bind to the AP-1 site. Fos- and Jun-related proteins bind to AP-1 sites with similar, although not identical, sequence specificities (24). ATF- and CREB-related proteins favor binding to the CRE site (9). However, most dimers formed both between members of the same family and between different families can bind to both AP-1 and CRE sites, although with different affinities (9).

The large number of different proteins that can bind to the AP-1 site provides the potential for elaborate regulatory specificity. Different heterodimeric complexes can have distinct effects at the same AP-1 site. Conversely, the same protein can have distinct effects at different AP-1 sites. The heterodimeric nature of the complex provides the opportunity for modulation of complex function through either component of the complex. This may allow integration of signals from separate signal transduction pathways that target different components of the complex. Thus, different heterodimeric complexes are likely to have distinct functional properties, and both components of the heterodimer are likely to contribute to the properties of the complex.

Fos and Jun family proteins operate in concert with other transcription factors to regulate transcription. This interplay is mediated in part through direct protein-protein interactions. Fos and Jun display regulatory interactions with the glucocorticoid, retinoid, estrogen, and thyroid receptors (see references in reference 17) as well as MyoD (3, 18), Oct-1 (29), and NF-ATp (12). Some interactions occur prior to DNA binding, such as the interaction between Fos and the glucocorticoid receptor, which selectively blocks DNA binding by Fos-Jun heterodimers (17). Other interactions occur on DNA, such as the interaction between NF-ATp and Fos-Jun, which bind cooperatively to the NF-AT site in the interleukin-2 promoter (12). In the osteocalcin gene, an AP-1 site overlaps the vitamin D response element and mediates repression by Fos and Jun (25). AP-1 sites are frequently found in complex regulatory elements containing binding sites for multiple unrelated transcription factors. Proteins binding to the AP-1 site are thus likely to regulate transcription cooperatively with other transcription factors. The transcriptional activity of Fos and Jun family proteins may therefore depend on the context of the AP-1 site and possibly the configuration of other transcription factors that can bind to the promoter region.

The proteins that bind to the AP-1 site do not form a single subfamily within the bZIP family on the basis of sequence similarities within the dimerization and DNA-binding domains (13). It is therefore possible that the prevalence of the AP-1 site as the recognition sequence for bZIP proteins is due to a structural complementarity between the bZIP DNA contact surface and the AP-1 site. The structure of the GCN4 bZIP dimerization and DNA-binding domain has been determined by X-ray crystallography (6). The monomers associate via a parallel coiled-coil dimerization interface (22) and contact the major groove of the recognition site as contiguous α helices (6). DNA contacts are mediated by a set of conserved amino acid residues that make contacts with specific bases and basic amino acid residues that make extensive contacts with the phosphodiester backbones of both strands. The contacts between the conserved amino acid residues and specific bases could explain the sequence specificity of GCN4 DNA binding in isolation. However, these amino acid residues are conserved throughout the bZIP protein family, regardless of binding site specificity.

* Corresponding author.

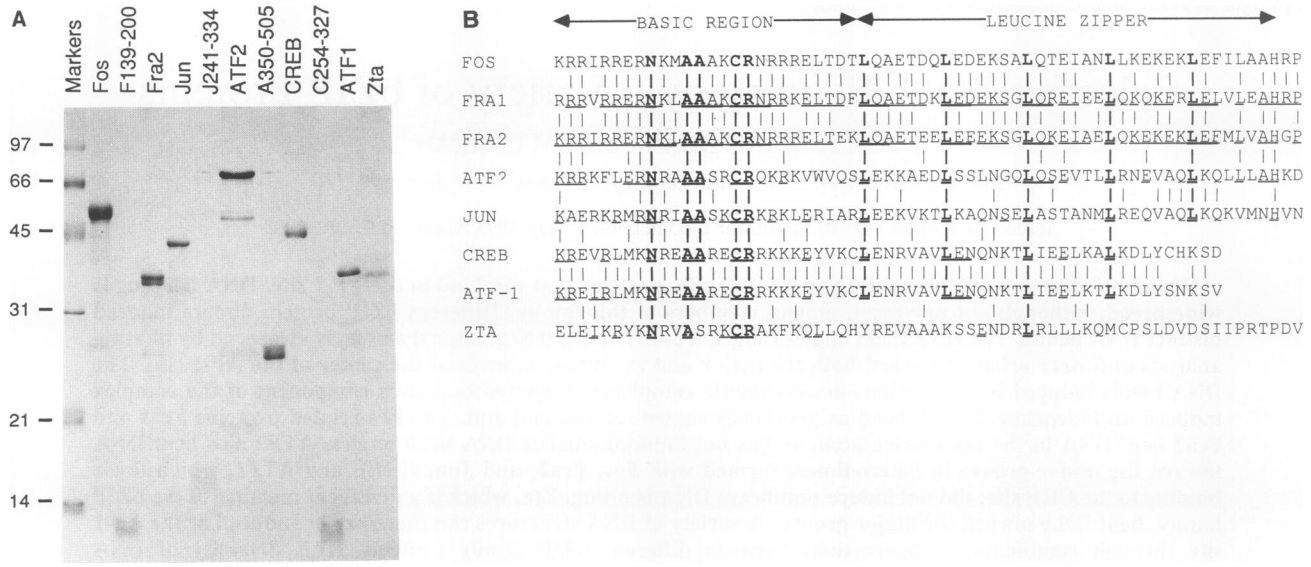

FIG. 1. Purified bZIP family proteins. (A) The purified proteins were resolved on a 15% polyacrylamide–sodium dodecyl sulfate gel and visualized by staining with Coomassie brilliant blue. The markers (Bio-Rad) were phosphorylase *b* (97 kDa), bovine serum albumin (66 kDa), ovalbumin (45 kDa), carbonic anhydrase (31 kDa), soybean trypsin inhibitor (21 kDa), and lysozyme (14 kDa). (B) Sequence similarities between the basic regions and leucine zippers of selected bZIP family proteins. Residues shared between each pair of adjacent sequences are connected by a line. Residues shared between each sequence and Fos are underlined. Residues shared among most bZIP family proteins are shown in boldface.

Therefore, the structural basis of DNA-binding specificity among other bZIP family members remains unclear.

We have previously investigated the effects of DNA binding by Fos-Jun heterodimers and Jun homodimers on the structure of the AP-1 site. Fos-Jun heterodimers and Jun homodimers bend DNA in opposite orientations (14, 15). Since these related proteins induce distinct changes in DNA structure, their DNA-binding domains are likely to adopt different structures upon DNA binding. Although the dimerization and DNA-binding domains of Fos and Jun are sufficient to induce DNA bending, domains outside of these regions modulate the DNA bend angle (14, 15). The DNA bends induced by these dimeric complexes represent the sum of independent DNA bends induced by the individual subunits. Thus, heterodimers between Fos and Jun that bend DNA in opposite orientations cause a smaller overall DNA bend angle than would heterodimers between proteins that induced equivalent DNA bends in the same orientation.

The DNA-bending properties of families of related proteins have been investigated in only a few cases. The POU family proteins Oct-1, Oct-2A, Oct-6, and Pit-1 induce DNA distortions, as determined by circular permutation analysis (30). However, only the Oct-1 POU domain has been investigated by phasing analysis. A modest mobility variation was observed in this assay, suggesting that Oct-1 induces a relatively small DNA bend angle. The helix-loop-helix proteins TFEB, TFE3, USF, Myc, and Max also induce DNA distortions, as determined by circular permutation analysis (7, 31). TFEB, TFE3, USF, Max, and Myc-Max dimers bend DNA in the same orientation (7), but Myc homodimers bend DNA in the opposite orientation (31), as determined by phasing analysis. However, the mobility variations induced by of all these proteins in phasing analysis are modest, suggesting that they induce relatively small DNA bend angles.

To test the hypothesis, predicted by the independent DNA bends model, that dimers formed by Fos and Jun family proteins generate an array of distinct DNA bends, we investigated DNA bending by different heterodimeric and homodimeric complexes. The DNA bend angles induced by different dimers were found to range from virtually 0 to greater than 40°, as determined by phasing analysis. Each protein induced a characteristic DNA bend angle and orientation that were generally independent of the dimerization partner. The AP-1 site may therefore represent a sequence element of unusual conformational flexibility. This flexibility could contribute to sequence-specific recognition of AP-1 sites by bZIP family proteins.

MATERIALS AND METHODS

Proteins. All proteins, with the exception of those used for the initial analysis of Fos- and Jun-related proteins (see Fig. 2), were expressed in *Escherichia coli* or insect cells and purified to >90% homogeneity (Fig. 1A). The expression and purification of Fos, F139-380, Jun, J225-334, and J241-334 have been described previously (1). F139-200 contains residues 139 to 200 of Fos with an amino-terminal MHHHHH HAST fusion peptide and was expressed and purified by the same methods. F139-200, J225-334, and J241-334 represent truncated proteins encompassing the leucine zipper dimerization and basic DNA-binding regions of Fos and Jun. Fra2 was cloned from a rat cDNA library and cloned into plasmid pDS56 with an MHHHHHH fusion peptide (25a). The protein was overexpressed and purified by nickel chelate affinity chromatography (1). The ATF2 expression vector (2) was a generous gift from J. Hoeffler, and ATF2 was purified by nickel chelate affinity chromatography under both native and denaturing conditions as previously described (17). Truncated ATF2 (A350-505), CREB, and truncated CREB (254-327) were a generous gift from J. Hoeffler and were purified as previously described (4, 11). ATF1, ATF4, and

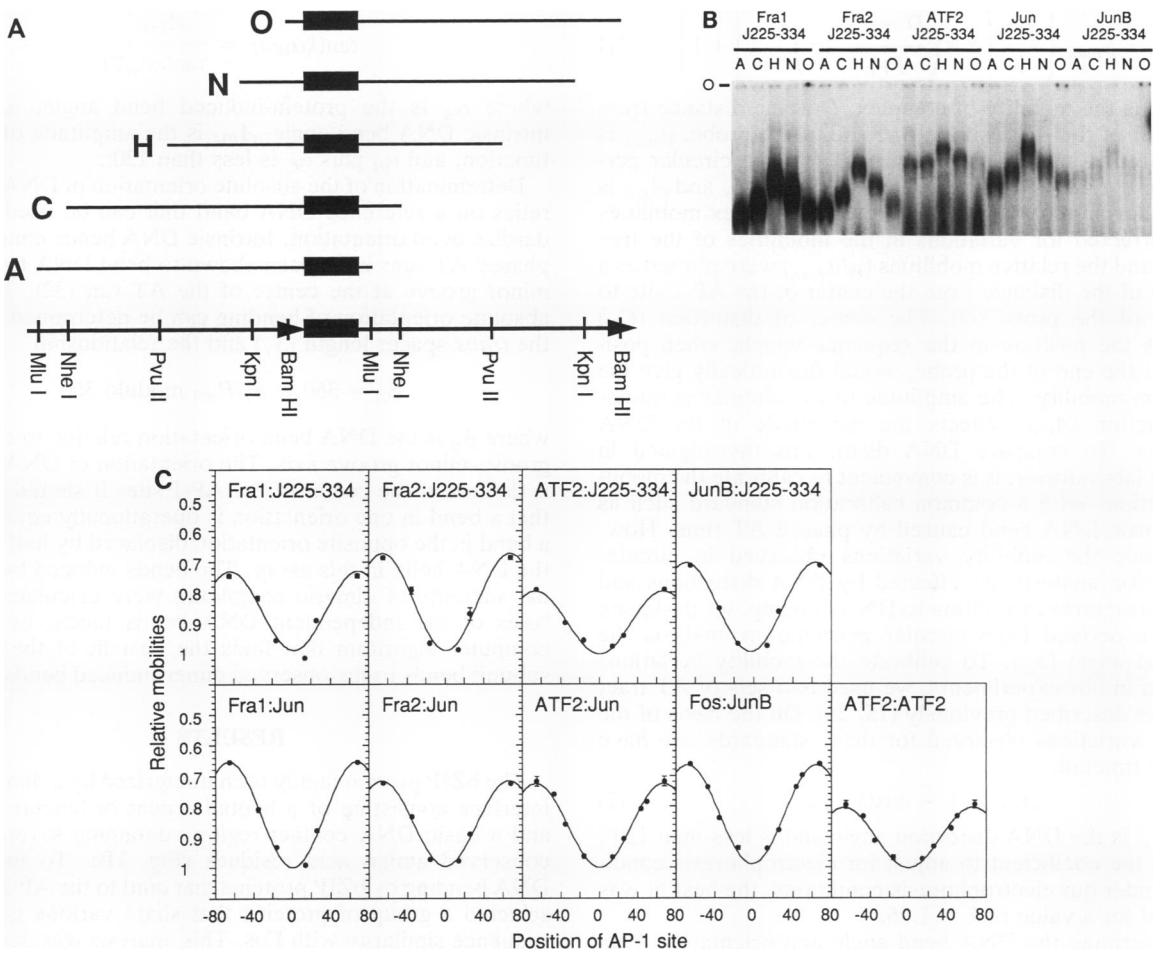

FIG. 2. Circular permutation analysis of DNA distortion by Fos- and Jun-related proteins. (A) The probes used in circular permutation analysis were generated by polymerase chain reaction amplification of a region of plasmid pTK401 containing an AP-1 site (closed box) flanked by tandem repeats of polylinker sequences followed by restriction enzyme cleavage at sites within the polylinker sequences (14). All probes were of the same length and contained different circular permutations of the same DNA sequences. (B) Fos, Fra1, Fra2, ATF2, Jun, and JunB were translated in vitro and incubated with an excess of truncated Jun (J225-334) protein purified from *E. coli*. The heterodimers were incubated with the circular permutation analysis probes, and the complexes were analyzed by polyacrylamide gel electrophoresis. The J225-334 homodimer is outside of the region shown in the figure. (C) The relative mobilities of complexes formed by the proteins indicated in each graph were normalized for slight differences in probe mobilities and plotted as a function of the position of the AP-1 site (15). The points are connected by the best fit of a cosine function (16). Standard deviations are indicated by vertical bars.

ATF6 were also kindly provided by J. Hoeffler and consist of the coding regions previously described (10) and were expressed in *E. coli* and purified as described for ATF2 (A350-505) and CREB (254-327) (11). Zta and the deletion derivative ZtaΔ25-141 were a generous gift from P. Lieberman and A. Berk and were purified as previously described (19). For the initial analysis (Fig. 2), Fos, Fra1, Fra2, ATF2, Jun, and JunB proteins were translated in a reticulocyte extract. The reticulocyte extract-translated proteins exhibited the same characteristics as proteins purified from *E. coli*; however, nonspecific DNA-binding activities in the extract interfered with further analysis.

Circular permutation and phasing analysis. The probes used for circular permutation and phasing analysis have been described (14). Briefly, the circular permutation analysis probes were all 133 bp in length and contained the AP-1 site at different positions relative to the ends of the probe. Circular permutation analysis probes that were identical to these, but contained a CRE site, were constructed as previously described (14). The phasing analysis probes were between 350 and 360 bp in length and contained an intrinsic DNA bend consisting of three phased AT tracts separated from the AP-1 site by spacers of different lengths. The distances between the centers of the intrinsic bends and the AP-1 sites were 21, 23, 26, 28, and 30 bp. The methods used for association of bZIP heterodimers, DNA binding, and polyacrylamide gel electrophoresis have been described previously (14, 15). To optimize the yield of heterodimers, the molar ratio of the proteins in the DNA-binding reaction mixture was initially varied, and the ratio that gave the maximum yield of heterodimer complexes was subsequently used. Under these optimized conditions, the majority of complexes were generally heterodimers.

Quantitation of DNA distortion and bending. To quantitate the magnitude of the DNA distortion from the variation in the mobilities of complexes during circular permutation analysis, we determined the best fit of the complex mobilities to the circular permutation function (15)

$$\mu = \mu_{max}\left\{\frac{A_{CP}}{2}\left[\cos\left(\frac{D - C_D}{P_{CP}}2\pi\right) - 1\right] + 1\right\} \quad (1)$$

where μ is the mobility of complex, D is the distance from the center of the AP-1 site to one end of the probe, μ_{max} is the theoretical maximum mobility, P_{CP} is the circular permutation period, C_D is the center of distortion, and A_{CP} is the circular permutation amplitude. The complex mobilities were corrected for variations in the mobilities of the free probes, and the relative mobilities (μ/μ_{max}) were plotted as a function of the distance from the center of the AP-1 site to the end of the probe (D). The center of distortion (C_D) indicates the position in the sequence which, when positioned at the end of the probe, would theoretically give the maximum mobility. The amplitude of the circular permutation function (A_{CP}) reflects the magnitude of the DNA distortion. To compare DNA distortions investigated in different laboratories, it is convenient to calibrate the mobility variations with a common calibration standard such as the intrinsic DNA bend caused by phased AT runs. However, since the mobility variations observed in circular permutation analysis are affected by DNA distortions and protein structures in addition to DNA bending, we designate the angle derived from circular permutation analysis the distortion angle (α_D). To calibrate the mobility variations observed in our experiments, we used two sets of AT tract standards described previously (15, 28). On the basis of the mobility variations observed for these standards, we have used the function

$$A_{CP} = 1 - \cos(k\alpha_D/2) \quad (2)$$

where α_D is the DNA distortion angle and is less than 120°, and k is the coefficient to adjust for electrophoresis conditions. Under our electrophoresis conditions, the best fit was observed for a value of $k = 1.06$.

To determine the DNA bend angle and orientation from the variation in the mobilities of complexes during phasing analysis, we determined the best fit of the complex mobilities to the phasing function (15)

$$\mu = \mu_{avg}\left\{\frac{A_{PH}}{2}\left[\cos\left(\frac{S - S_T}{P_{PH}}2\pi\right)\right] + 1\right\} \quad (3)$$

where μ is the mobility of complex, S is the distance from the center of the binding site to the center of the intrinsic bend, μ_{avg} is the theoretical average mobility, P_{PH} is the phasing period, S_T is the *trans* center-to-center distance, and A_{PH} is the phasing amplitude. The complex mobilities were corrected for variations in the mobilities of the free probes and the relative mobilities (μ/μ_{avg}) were plotted as a function of the distance from the center of the binding site to the center of the intrinsic bend (S). The *trans* center-to-center distance (S_T) indicates the distance at which the intrinsic and protein-induced bends are predicted to counteract each other perfectly, causing maximal complex mobility. The amplitude of the phasing function represents the difference between the relative mobilities of complexes in which the intrinsic and protein-induced bends cooperate and counteract each other. Thus, the protein-induced bend angle can be calculated from the amplitude of the phasing function (A_{PH}) and the known DNA bend angle (α_C) of the intrinsic bend placed in tandem with the protein-induced bend. We have derived (15, 16) a mathematical relationship between these quantities on the basis of the assumption that the mobility of a DNA fragment containing two closely spaced DNA bends is determined by the overall DNA bend angle:

$$\tan(k\alpha_B/2) = \frac{A_{PH}/2}{\tan(k\alpha_c/2)} \quad (4)$$

where α_B is the protein-induced bend angle, α_C is the intrinsic DNA bend angle, A_{PH} is the amplitude of phasing function, and α_B plus α_C is less than 120°.

Determination of the absolute orientation of DNA bending relies on a reference DNA bend that can be used to standardize bend orientation. Intrinsic DNA bends consisting of phased AT runs have been shown to bend DNA toward the minor groove at the center of the AT run (32). Thus, the absolute orientation of bending can be determined by using the *trans* spacer length (S_T) and the relationship

$$\beta_B = 360 \times S_T/P_{PH} \text{ modulo } 360 \quad (5)$$

where β_B is the DNA bend orientation relative to the major groove-minor groove axis. The orientation of DNA bending is defined at the center of the AP-1 site. It should be noted that a bend in one orientation is operationally equivalent to a bend in the opposite orientation displaced by half a turn of the DNA helix in this assay. The bends induced by individual subunits of dimeric complexes were calculated on the basis of the independent DNA bends model by using a computer algorithm that finds the best fit of the sums of subunit bends to the observed dimer-induced bends (15, 16).

RESULTS

The bZIP protein family is characterized by a dimerization interface consisting of a heptad repeat of leucine residues and a basic DNA contact region containing several highly conserved amino acid residues (Fig. 1B). To investigate DNA bending by bZIP proteins that bind to the AP-1 site, we selected a group of proteins that share various degrees of sequence similarity with Fos. This analysis was designed to determine how widespread DNA bending was within the bZIP protein family and to understand the relationship between DNA bending and primary structure among these proteins.

DNA bending by Fos-related proteins. Several proteins that share particularly close sequence similarity with the basic and leucine zipper regions of Fos have been identified (Fig. 1B, Fra-1 and Fra-2) (5, 21). These proteins also exhibit a more limited sequence similarity in amino- and carboxy-terminal regions. To investigate DNA bending by these Fos-related proteins, we conducted circular permutation and phasing analyses of complexes formed by Fra1 with Jun and Fra2 with Jun and ATF2 proteins. Circular permutation analysis of Fra1 and Fra2 heterodimers formed with full-length and truncated Jun indicated that all heterodimers induced structural distortions when bound to the AP-1 site (Fig. 2). Complexes containing ATF2 or JunB also induced a mobility variation. The center of distortion was located close to the center of the AP-1 site for all complexes. However, circular permutation analysis does not specifically detect DNA bends, as it is sensitive to other structural distortions (8, 14, 15). Thus, these results only suggest that complexes containing Fra1 or Fra2 induce structural distortions.

To determine whether Fra1 and Fra2 induce directed DNA bends and to determine the orientation of such bends, we used phasing analysis to study complexes formed by Fra1 with Jun and Fra2 with Jun and ATF2 proteins. Fra2 in association with full-length Jun induced no directed DNA bending, whereas Fra2 dimerized with truncated Jun induced a directed DNA bend (Fig. 3). Fra2 heterodimers

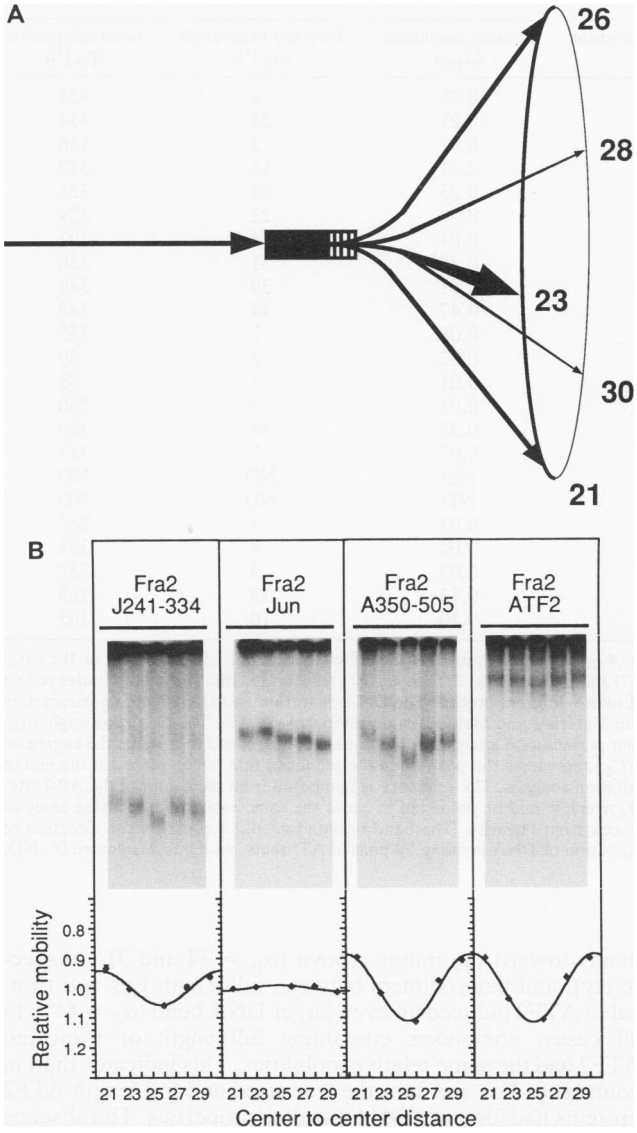

FIG. 3. Phasing analysis of DNA bending by Fra2 heterodimers formed with Jun, truncated Jun (J241-334), ATF2, and truncated ATF2 (A350-505). (A) The probes used in phasing analysis were generated by polymerase chain reaction amplification of a region of plasmids pTK401-21, pTK401-23, pTK401-26, pTK401-28, and pTK401-30 that contains an AP-1 site (closed box) separated by spacers of different lengths (striped box) from an intrinsic DNA bend consisting of three phased AT runs (14). The names of the probes indicate the distance in base pairs between the centers of the AP-1 site and the intrinsic bend. With the exception of the different spacer lengths, all probes were of the same size and contained the same DNA sequences. (B) The proteins indicated in each frame were incubated to form heterodimers. The heterodimers were incubated with phasing analysis probes, and the complexes were analyzed by polyacrylamide gel electrophoresis. The relative mobilities of complexes formed by the proteins indicated in each graph were normalized for slight differences in probe mobilities and plotted as a function of the distance between the centers of the AP-1 site and the intrinsic DNA bend (15). The points are connected by the best fit of a cosine function (16). Standard deviations are indicated by vertical bars.

formed with either full-length or truncated ATF2 also induced directed DNA bends. The slowest complex mobility is observed when the intrinsic and protein-induced DNA bends cooperate to produce the maximum DNA bend angle, and the fastest complex mobility is observed when the two bends counteract each other to produce the minimum DNA bend angle (14, 15). Thus, the orientation of DNA bending can be determined from the maxima and minima of the mobility pattern in combination with the previously determined orientation of intrinsic DNA bending (Table 1). Fra2 heterodimers formed with truncated Jun, full-length ATF2, or truncated ATF2 all induced DNA bends toward the minor groove at the center of the AP-1 site. The orientation of DNA bending in these complexes (β_B = 322 to 342°) was virtually identical to that observed in the Fos-Jun heterodimer complex (β_B = 333°) (15). The variation in the relative mobilities of the complexes in phasing analysis is a function of the magnitude of the directed DNA bend angle (15). Thus, the magnitudes of the respective DNA bend angles can be calculated from this mobility variation (Table 1). The DNA bend angle induced by Fra2 heterodimers formed with truncated Jun (α_B = 11°) was similar to those induced by truncated Fos-Jun heterodimers and truncated Jun homodimers (α_B = 12°) (15). However, the DNA bend angle induced by Fra2 heterodimers formed with full-length or truncated ATF2 (α_B = 22°) was closer to those induced by full-length Fos-Jun heterodimers and Jun homodimers (α_B = 23 and 27°, respectively) (15). Fra1 heterodimers formed with full-length and truncated Jun also induced bending toward the minor groove. The DNA bend angles induced by Fra1 heterodimers formed with full-length or truncated Jun (α_B = 8 and 21°, respectively) were larger than those induced by the corresponding complexes formed by Fra2 but smaller than those induced by the corresponding Fos complexes (Table 1) (15).

Previously we proposed an independent DNA bends model for DNA bending by Fos-Jun heterodimers (15). According to this model, each component of a dimer induces an independent DNA bend. The DNA bend induced by each protein is constant and unaffected by the dimerization partner. The overall bend induced by a dimeric complex is therefore the vector sum of the bends induced by each component of the complex. The results from our studies of Fra1 and Fra2 complexes with full-length and truncated Jun and ATF2 proteins are consistent with this independent DNA bends model. The absence of a directed DNA bend in the Fra2-Jun complex can be explained if Fra2 and Jun induce DNA bends of similar magnitudes but of opposite orientations. Since our previous results indicate that Jun bends DNA toward the major groove (14, 15), Fra2 must bend DNA toward the minor groove. This is consistent with the bend toward the minor groove induced by the Fra2 heterodimer with truncated Jun, which induces a smaller bend angle than full-length Jun (14, 15). The DNA bends induced by Fra2 heterodimers formed with full-length and truncated ATF2 proteins predict that these proteins also bend DNA toward the minor groove. This prediction is consistent with the DNA-bending properties of other ATF2 heterodimers (see below). The bend toward the minor groove induced by Fra1-Jun heterodimers and the larger bend induced by Fra1 heterodimers formed with truncated Jun indicate that Fra1 also bends DNA toward the minor groove. Thus, the Fra1 and Fra2 proteins, which share close sequence similarity with the DNA contact region of Fos, also share the same DNA bend orientation. However, the three proteins differ in the magnitudes of their DNA bend

TABLE 1. DNA distortion and bending by different bZIP protein dimers[a]

Protein dimer	Circular permutation analysis			Phasing analysis		
	Circular permutation amplitude (A_{CP})	Distortion angle (α_D [°])	Center of distortion (C_D)	Phasing amplitude (A_{PH})	Directed bend angle (α_B [°])	Bend orientation (β_B [°])
Fra1-Jun	0.35	90	1	0.08	8	328
Fra1–J225-334	0.26	78	3	0.21	21	334
Fra2-Jun	0.28	80	0	0.02	2	136
Fra2–J241-334	0.33	87	1	0.11	11	342
Fra2-ATF2	ND	ND	ND	0.23	22	322
Fra2–A350-505	ND	ND	ND	0.22	22	329
A350-505	0.43	104	2	0.04	4	297
A350-505–F139-200	0.42	103	3	0.32	31	336
A350-505–F139-380	ND	ND	ND	0.41	39	348
A350-505–Fos	ND	ND	ND	0.47	44	342
A350-505–J241-334	0.34	91	0	0.08	7	355
A350-505–J91-334	ND	ND	ND	0.02	2	89
A350-505–Jun	ND	ND	ND	0.01	1	98
ATF2	0.20	67	0	0.03	3	260
ATF2–F139-200	ND	ND	ND	0.35	34	320
ATF2–J241-334	ND	ND	ND	0.07	7	313
ATF2–J225-334	0.21	68	1	ND	ND	ND
ATF2-Jun	0.27	80	1	ND	ND	ND
CREB	0.49	111	0	0.03	3	267
CREB 254-327	0.10	49	1	0.04	4	354
ATF1	0.19	67	−2	0.03	3	332
Zta	0.36	95	1	0.13	13	163
ZtaΔ25-141	0.13	56	10	0.10	10	165

[a] The amplitudes of the circular permutation functions (A_{CP}) and phasing functions (A_{PH}) were determined, as described in Materials and Methods, on the basis of the mobilities of the various complexes during circular permutation (Fig. 2, 4, and 7) and phasing (Fig. 3, 5, 6, and 8) analysis (15, 16). These amplitudes reflect the degree of variation in the mobilities of the complexes when each dimer is bound to the different probes. The DNA distortion and DNA-bending parameters were determined from the circular permutation and phasing functions, as described in Materials and Methods and previously (15, 16). The distortion angle (α_D) is the intrinsic DNA bend angle that would cause the same mobility variation in circular permutation analysis as the protein complex and represents the aggregate effects of DNA and protein structure on complex mobility. The center of distortion (C_D) represents the position in the sequence that, when placed at the end of the probe, would theoretically yield the maximum complex mobility in circular permutation analysis. The sequence is numbered from the center of the AP-1 site, which is designated 0. The directed bend angle (α_B) is the intrinsic DNA bend angle, which would be predicted to cause the same variation in phasing analysis as the protein complex and represents the average directed deviation of the helix axis from linearity. The bend orientation (β_B) represents the direction of protein-induced DNA bending defined at the center of the AP-1 site relative to the direction of DNA bending by phased AT tracts, which is designated 0°. ND, not determined.

angles; Fos induces the largest bend, followed by Fra1 and Fra2.

DNA bending by ATF2 complexes. ATF2 is a particularly interesting member of the Fos- and Jun-related protein family (10, 20), since its basic region shares more sequence similarity with the Fos family of proteins whereas its leucine zipper is more similar to that of the Jun family (Fig. 1B). It forms heterodimers promiscuously with members of both the Fos and the Jun families as well as homodimers. Analysis of the DNA-bending properties of ATF2 heterodimers formed with different Fos and Jun proteins provided a stringent test of the independent DNA bends model. Circular permutation analysis of full-length ATF2 (Fig. 2), truncated ATF2, and truncated ATF2 heterodimers formed with truncated Fos and Jun proteins (Fig. 4) indicated that all complexes induced structural distortions.

To determine whether any of these complexes induced directed DNA bends, we studied the various complexes by phasing analysis (Fig. 5). Neither full-length nor truncated ATF2 homodimers induced significant directed DNA bending (α_B = 3 and 4°, respectively). Heterodimers between full-length or truncated ATF2 and truncated Jun induced a small bend (α_B = 7°) toward the minor groove. Heterodimers between truncated ATF2 and either full-length Jun or a Jun derivative (J91-334) with DNA-bending properties similar to those of Jun induced no significant bending (α_B = 1 and 2°, respectively). In contrast, heterodimers between full-length or truncated ATF2 and truncated Fos induced large DNA bends toward the minor groove (α_B = 34 and 31°, respectively), and heterodimers between full-length Fos and truncated ATF2 induced an even larger DNA bend (α_B = 44°). In all cases, complexes containing full-length or truncated ATF2 had the same relative mobilities. This indicates that, in contrast to Fos and Jun, the truncated and full-length ATF2 proteins had identical DNA-bending properties. The absence of DNA bending in complexes containing truncated ATF2 and full-length Jun and bends toward the minor groove induced by complexes containing truncated or full-length ATF2 and truncated Jun suggest that ATF2 bends DNA toward the minor groove. This is consistent with the large DNA bends induced by heterodimers containing full-length or truncated ATF2 and truncated Fos and the even larger DNA bend caused by truncated ATF2 heterodimers formed with full-length Fos. The bends induced by full-length and truncated ATF2 heterodimers formed with Fra2 are also consistent with ATF2 bending toward the minor groove (see above). The DNA bend angles induced by Fos and Fra2 dimerized with ATF2 are larger than the DNA bend angles induced by the same proteins dimerized with Jun. This is due to the different interactions between the two bends in these complexes. Whereas Jun counteracts DNA bending by Fos and Fra2, ATF2 cooperates with Fos and Fra2 to increase the overall DNA bend angle.

ATF2 homodimers induced little or no DNA bending. Several explanations may account for this apparent contradiction to the independent DNA bends model. First, the

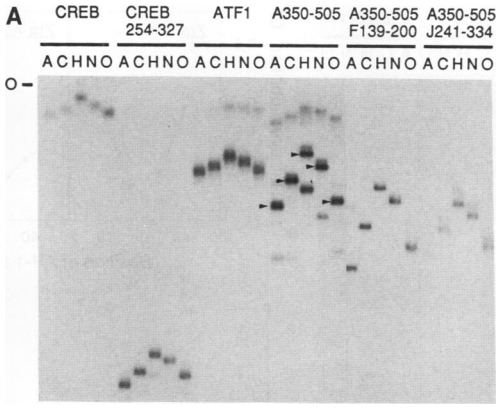

FIG. 4. Circular permutation analysis of DNA distortion by CREB, ATF1, and truncated ATF2 (A350-505) homodimers and A350-505 heterodimers formed with truncated Fos (F139-200) and truncated Jun (J241-334). (A) The proteins indicated above the lanes were incubated to form homo- and heterodimers. The heterodimers were incubated with DNA fragments and the complexes were analyzed as in Fig. 2B. Truncated ATF2 (A350-505), and to a lesser extent CREB 257-327 and ATF1, homodimers were found to form multiple occupancy complexes at higher protein concentrations. The arrowheads indicate the positions of the singly occupied complexes. A variable ratio of a higher-mobility complex was also observed. This may represent a proteolytic fragment generated during the experiment or a conformational isomer, such as we have previously observed for Fos and Jun (16). (B) The relative complex mobilities were normalized and plotted as in Fig. 2C.

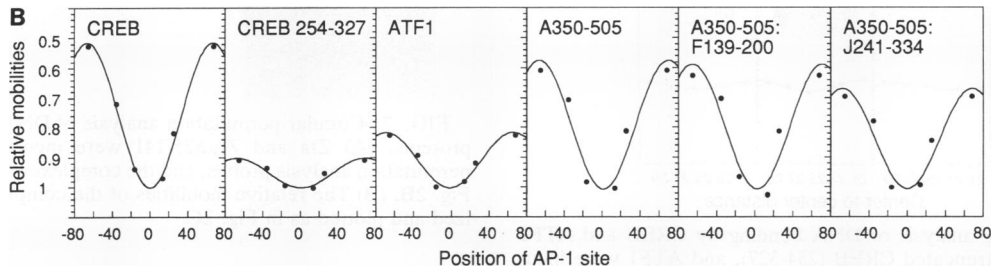

phasing between the two bends in the ATF2 homodimer complex may be different from that in the heterodimer complexes. Bends induced by subunits of dimeric complexes are additive if the two bends are in phase. Likewise, a subunit will contribute identically to DNA bending in different dimeric complexes only if the phasing between the bends is constant in all complexes. Thus, the bends induced by different Fos and Jun family members are additive in different complexes only if the leucine zipper dimerization interface has a constant geometry. Since ATF2 homodimers favor binding to the CRE site, we suggest that the leucine zipper in this complex has a geometry different from that of complexes that favor binding to the AP-1 site. It is therefore possible that the DNA bends induced by the two subunits of the ATF2 homodimer counteract each other. Second, ATF2 bound to different AP-1 half-sites may have different effects on DNA structure. To test this possibility, we examined DNA distortion by truncated ATF2 at six variants of the

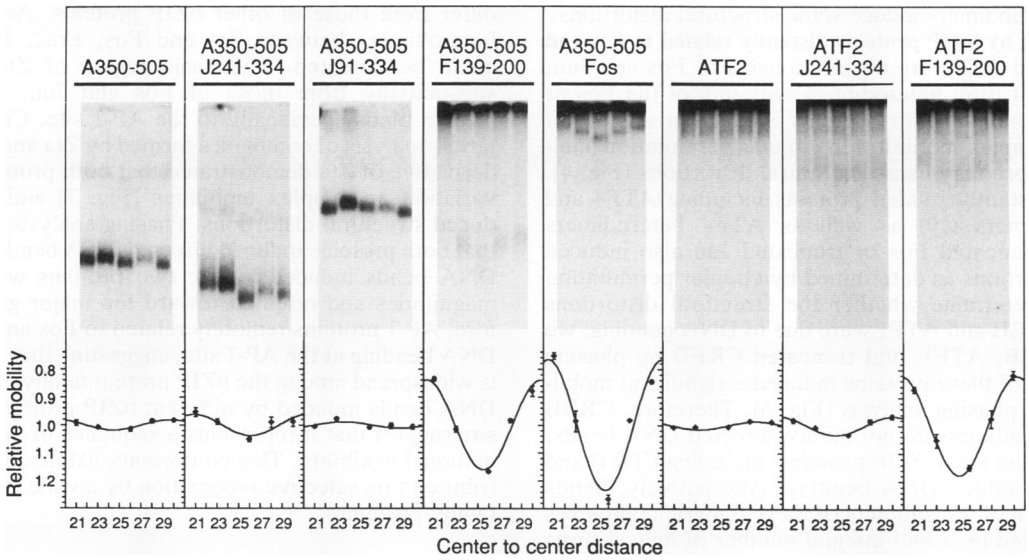

FIG. 5. Phasing analysis of DNA bending by ATF2 and truncated ATF2 (A350-505) homodimers and heterodimers formed with Fos and Jun proteins. The proteins indicated in each frame were incubated to form homo- and heterodimers, which were incubated with the phasing analysis probes, and the complexes were analyzed as in Fig. 3. Weak binding by purified full-length ATF2 protein was observed as previously described (2). The ATF2 homodimer migrated a very short distance in the gel, and thus it is difficult to determine the relative complex mobilities accurately.

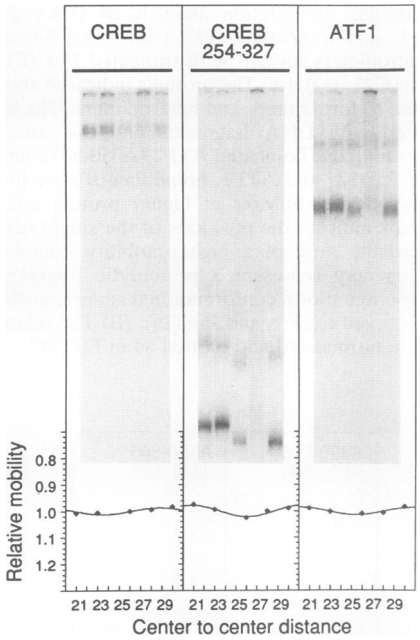

FIG. 6. Phasing analysis of DNA bending by CREB and ATF1 proteins. CREB, truncated CREB (254-327), and ATF1 were incubated with phasing analysis probes and the complexes were analyzed as in Fig. 3. Probe 28 used in this experiment migrated aberrantly.

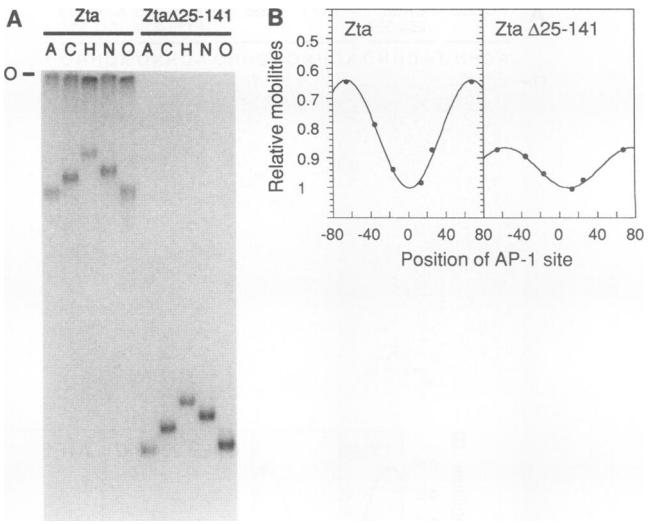

FIG. 7. Circular permutation analysis of DNA distortion by Zta proteins. (A) Zta and ZtaΔ25-141 were incubated with circular permutation analysis probes, and the complexes were analyzed as in Fig. 2B. (B) The relative mobilities of the complexes were normalized and plotted as in Fig. 2C.

AP-1 site containing different half-site sequences. There was no significant difference in the DNA distortions induced by ATF2 at these sites, and therefore ATF2 likely induces the same DNA structural change at both half-sites. Finally, ATF2 may adopt a different conformation in the homodimer that does not bend DNA. Although we cannot exclude this possibility, we favor the first interpretation since both truncated and full-length ATF2 homodimers cause a large variation in complex mobilities in circular permutation analysis, suggesting that the homodimers induce some structural distortions.

DNA bending by bZIP proteins distantly related to Fos and Jun. CREB and ATF1 are distant cousins of Fos and Jun, and they do not form heterodimers with any of the Fos or Jun family proteins. Both proteins induced a significant variation in complex mobilities in circular permutation analysis and therefore may cause structural distortions (Fig. 4). Other more distantly related proteins including ATF4 and ATF6 homodimers (10) as well as ATF4 heterodimers formed with truncated Fos or truncated Jun also induced structural distortions as determined by circular permutation analysis. To determine whether the structural distortions induced by CREB and ATF1 were due to DNA bending, we examined CREB, ATF1, and truncated CREB by phasing analysis. None of these proteins induced a significant mobility variation in phasing analysis (Fig. 6). Therefore, CREB and ATF1 homodimers do not induce directed DNA bends. This suggests that some bZIP proteins, including CREB and ATF1, do not induce DNA bending. Alternatively, bends induced by each of the subunits of these dimeric complexes may be separated by a half-integral number of helical turns and may therefore cancel each other.

CREB, ATF1, and ATF2 bind preferentially to the CRE site, which differs from the AP-1 site by the insertion of a single base pair at the center of the site. To investigate if there might be a difference in DNA bending by these proteins at the AP-1 and CRE sites, we examined the effects of these proteins at the CRE site by circular permutation analysis. There were no differences in the mobility variations induced by these proteins at AP-1 and CRE sites in circular permutation analysis. These results suggest that there is no difference in the effects of CREB, ATF1, and ATF2 on DNA structure at the AP-1 or CRE sites.

To investigate whether AP-1 binding proteins only remotely related to Fos and Jun induced DNA bending, we examined DNA bending by the Epstein-Barr virus transcription factor Zta (19). Zta is a divergent member of the bZIP family, since it lacks the canonical heptad repeat of leucine residues, and its dimerization interface is therefore likely to differ from those of other bZIP proteins. Accordingly, no heterodimers between Zta and Fos, Fra2, Jun, or ATF2 could be detected. The basic region of Zta also differs substantially from those of Fos and Jun; however, the protein binds specifically to the AP-1 site. Circular permutation analysis of complexes formed by Zta and by a deletion derivative of Zta demonstrated that both proteins induced a variation in complex mobilities (Fig. 7) and therefore induced structural distortions. Phasing analysis demonstrated that both proteins induced directed DNA bends (Fig. 8). The DNA bends induced by the two proteins were of similar magnitudes and oriented toward the major groove. Therefore, AP-1 proteins remotely related to Fos and Jun induced DNA bending at the AP-1 site, suggesting that DNA bending is widespread among the bZIP protein family. The variety of DNA bends induced by different bZIP proteins at the AP-1 site suggest that it represents a sequence of unusual conformational flexibility. This conformational flexibility may contribute to its selective recognition by a wide variety of bZIP family proteins.

DISCUSSION

Different dimeric complexes formed between bZIP family proteins can induce a variety of topologically distinct DNA structures at the AP-1 site. The DNA bend angles induced by

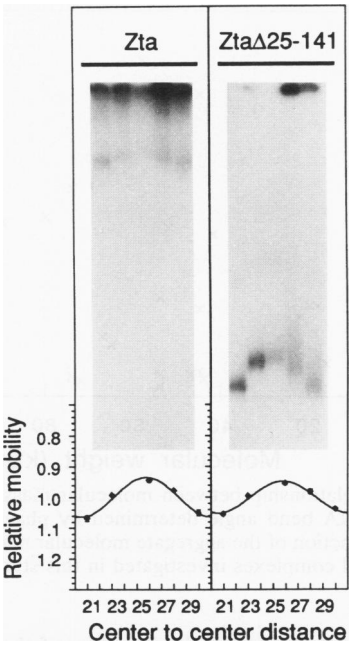

FIG. 8. Phasing analysis of DNA bending by Zta proteins. Zta and ZtaΔ25-141 were incubated with the phasing analysis probes, and the complexes were analyzed as in Fig. 3.

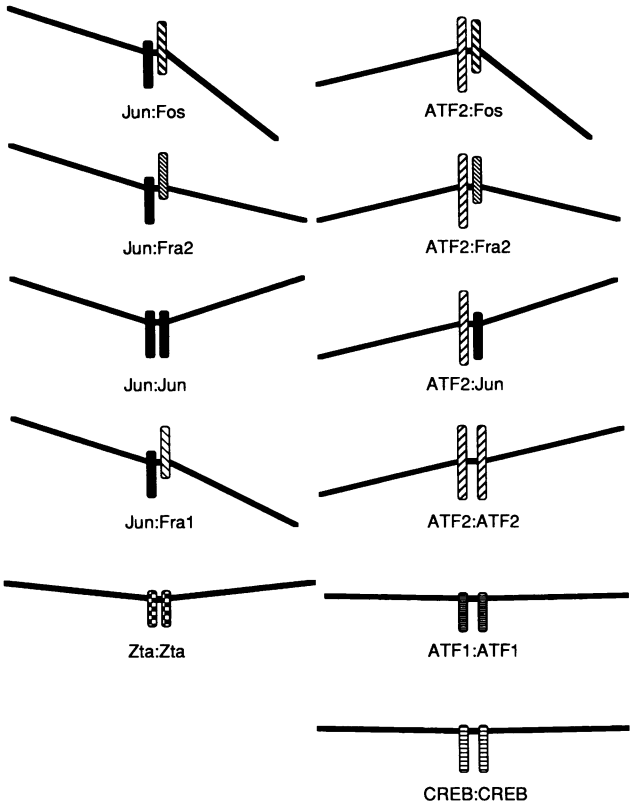

FIG. 9. Schematic diagram of DNA bending by Fos and Jun family proteins. The DNA bends induced by each of the individual proteins were calculated on the basis of the independent DNA bends model (15). The DNA bends are shown in projection approximately in the orientation of the major groove-minor groove axis at the center of the AP-1 site. The major groove is pointing up, and the minor groove is pointing down. The DNA bends predicted on the basis of the independent DNA bends model agree closely with the DNA bends observed for each heterodimeric complex (Table 1). The altered conformation of proteins that favor binding to the CRE site (see text) is represented by a larger separation between the subunits in the complex.

these complexes range from no detectable DNA bending to greater than 40°, as determined by phasing analysis. Therefore, DNA bending may confer specificity to the large family of complexes that can bind to the AP-1 site. Differences in AP-1 site bending may alter the interactions between transcription factors bound to flanking sequences. Bending may also promote or inhibit DNA binding by proteins that recognize overlapping or adjacent DNA sequence elements. Intrinsic DNA bends have been shown to markedly influence DNA binding by several eukaryotic transcription factors (23, 26). Conversely, constraints on DNA curvature at a particular AP-1 site, imposed by other proteins binding to overlapping or adjacent sites, may specify the Fos and Jun family members that can bind to the site. Such a constraint may be imposed by the wrapping of DNA in nucleosomes, which causes it to assume a fixed curvature. Such nucleosomal DNA can be bound only by a subset of transcription factors (27), which may be related to their ability to bind curved DNA. Thus, differences in the DNA structures induced by Fos and Jun family members may contribute to their regulatory specificity.

The variety of structures adopted by the AP-1 site when bound by different Fos and Jun family proteins suggests that it represents a sequence of unusual structural flexibility. This structural flexibility may contribute to the recognition of the AP-1 site by bZIP proteins that induce changes in DNA structure. Conversely, this diversity of DNA structures suggests that the DNA contact surfaces of different AP-1 binding proteins may adopt different structures upon DNA binding, as originally suggested in our flexible-hinge model (16). However, the orientations of DNA bending induced by bZIP family proteins are limited to directions that closely parallel the major groove-minor groove axis at the center of the AP-1 site. This restriction may be determined by either conformational constraints of the AP-1 site or the mechanism of DNA bending by bZIP family proteins. The observation that Zta, which is a highly divergent bZIP family member, bends DNA suggests that DNA bending is widespread among the bZIP protein family. Nevertheless, DNA bending is not universal, as demonstrated by our observations that neither CREB nor ATF1 bends DNA. This structural flexibility may be facilitated by interactions between arginine and lysine side chains and the phosphodiester backbone, as observed in the crystal structure of GCN4 (6). The long aliphatic side chains of arginine and lysine may permit recognition of a variety of AP-1 site conformations. This flexibility may allow other residues in the basic region, as well as other regions of the proteins, to alter the structure of the AP-1 site without disrupting these contacts with the phosphodiester backbone.

The DNA bends induced by virtually all complexes we have investigated are consistent with the independent DNA bends model (15). Thus, each monomer appears to induce an independent DNA bend which is unaffected by the dimerization partner. This is graphically illustrated in Fig. 9. The bend induced by each protein remains constant in all dimers formed by that protein. Different dimers induce distinct DNA bends by virtue of the different combinations of

monomer-induced bends. The DNA bends determined on the basis of the independent DNA bends model are in close agreement with the primary structure relationships of the various proteins. The Fos-related proteins Fra1 and Fra2 bend DNA in the same orientation as Fos but induce smaller DNA bend angles. The ATF2 protein also induced a bend in the same orientation as Fos, consistent with the closer sequence similarity between the basic region of ATF2 and the basic region of Fos, compared with the basic region of Jun. However, by virtue of the closer similarity of the leucine zipper of ATF2 to that of Jun, it can associate with Fos to form a dimer of two proteins that bend DNA toward the minor groove, resulting in a large DNA bend in this orientation.

CREB and ATF1 are closely related to each other but more distantly related to Fos and Jun. Homodimers of both of these proteins did not induce directed DNA bending. This suggests that dimers that favor binding to the CRE site may adopt a conformation different from those that favor binding to the AP-1 site. This conformation may involve an altered geometry at the junction between the leucine zipper and the basic region as suggested on the basis of the GCN4 crystal structure (6). This lack of DNA bending among proteins that favor binding to the CRE site may also account for the absence of DNA bending by ATF2 homodimers. Therefore, the dimerization interface between bZIP family proteins may also affect DNA bending.

We have previously reported that regions outside of the leucine zippers and basic regions influence DNA bending by Fos and Jun (14, 15). Our results here demonstrate that complexes containing full-length versus truncated Fos or Jun proteins dimerized with other bZIP proteins induce distinct DNA bends, consistent with our previous conclusions. However, full-length and truncated ATF-2, CREB, and Zta had similar DNA-bending properties. Although several of these truncated proteins extend beyond the bZIP region, it appears that there are both bZIP proteins for which the bZIP region fully determines their DNA-bending properties and bZIP proteins for which additional regions contribute to DNA bending. Fra1 and Fra2 induced smaller DNA bend angles in the same orientation as Fos. This difference in DNA bend angles is most likely due to the absence or only partial conservation of a region that increases DNA bending in Fos (16a). Consistent with this interpretation, the DNA bend angles induced by Fra1 and Fra2 are similar to that induced by a truncated Fos protein encompassing only the dimerization and DNA-binding domains (14, 15).

There is a frequent misconception that protein-induced DNA bending is related to the molecular mass of the protein. To dispel this prejudice, we plotted the DNA bend angles of all complexes we investigated as a function of the molecular mass of the complex (Fig. 10). There was no significant correlation ($r < 0.1$) between DNA bending and the molecular mass of the complex. The ATF2 homodimer was the largest complex investigated but did not induce significant DNA bending, whereas the F139-200–A350-505 heterodimer, which was one of the smallest complexes tested, induced one of the largest DNA bend angles. Thus, determination of DNA bend angles by phasing analysis is not significantly affected by protein molecular mass.

Our results also demonstrate that circular permutation analysis is not a reliable method for the determination of directed DNA bends. Several complexes were characterized in this as well as in previous (8, 15) studies that did not induce a directed DNA bend as determined by phasing analysis but did cause a significant mobility variation in circular permutation analysis. In some of these cases, such as the Fra2-Jun heterodimer, the individual monomers induced counteracting DNA bends of similar magnitudes, generating a "jog" in DNA. This DNA jog, or DNA flexibility associated with this structure (15), may account for some of the mobility variation in circular permutation analysis. In several cases, including CREB and Zta, the full-length and the truncated proteins induced the same DNA bend angle as determined by phasing analysis, but the full-length protein induced a much larger variation in circular permutation analysis. In these, as well as in other, cases, extended protein domains are likely to contribute to the mobility variation in circular permutation analysis.

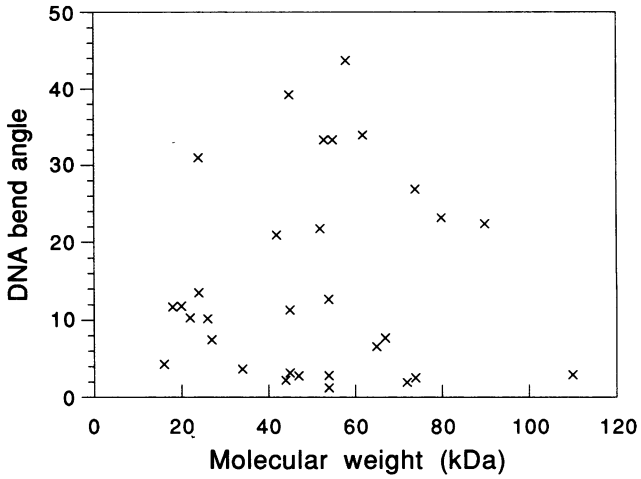

FIG. 10. Relationship between molecular mass and DNA bend angle. The DNA bend angle determined by phasing analysis was plotted as a function of the aggregate molecular mass of the dimeric complex for all complexes investigated in this study.

Our results indicate that DNA bending may serve as a specificity determinant among members of protein families with closely related DNA-binding specificities. Transcription activation requires interactions between some proteins bound to upstream regulatory elements and the general initiation complex. The initiation complex itself may contact multiple sequence elements, which would require looping of intervening sequences. Such DNA looping can be facilitated by proteins that induce bending in the intervening DNA. Proteins that induce different DNA bend angles and orientations may direct the assembly of initiation complexes with distinct structural and functional properties. Further studies of the function of DNA bending during assembly of initiation complexes and during transcription initiation are required to elucidate the role of transcription factor-induced DNA bending in the regulation of gene expression.

ACKNOWLEDGMENTS

T.K.K. is supported by a postdoctoral fellowship from The Helen Hay Whitney Foundation.

We thank Jim Hoeffler and Paul Lieberman for generous gifts of purified proteins.

REFERENCES

1. **Abate, C., D. Luk, and T. Curran.** 1991. Transcriptional regulation by Fos and Jun in vitro: interaction among multiple activator and regulatory domains. Mol. Cell. Biol. **11**:3624–3632.
2. **Abdel-Hafiz, H. A., L. E. Heasley, J. M. Kyriakis, J. Avruch,**

D. J. Kroll, G. L. Johnson, and J. P. Hoeffler. 1992. Activating transcription factor-2 DNA binding activity is stimulated by phosphorylation catalyzed by p42 and p54 microtubule-associated protein kinases. Mol. Endocrinol. **6**:2079–2089.

3. **Bengal, E., L. Ransone, R. Scharfmann, V. J. Dwarki, S. J. Tapscott, H. Weintraub, and I. M. Verma.** 1992. Functional antagonism between c-Jun and MyoD proteins: a direct physical association. Cell **68**:507–519.
4. **Chen, C.-Y., D. H. Bessesen, S. M. Jackson, and J. P. Hoeffler.** 1991. Overexpression and purification of transcriptionally competent CREB from recombinant baculovirus. Prot. Exp. Purif. **2**:402–411.
5. **Cohen, D. R., and T. Curran.** 1988. *fra-1*: a serum-inducible, cellular immediate-early gene that encodes a Fos-related antigen. Mol. Cell. Biol. **8**:2063–2069.
6. **Ellenberger, T. E., C. J. Brandl, K. Struhl, and S. C. Harrison.** 1992. The GCN4 basic region leucine zipper binds DNA as a dimer of uninterrupted α helices: crystal structure of the protein-DNA complex. Cell **71**:1223–1237.
7. **Fisher, D. E., L. A. Parent, and P. A. Sharp.** 1992. Myc/Max and other helix-loop-helix/leucine zipper proteins bend DNA toward the minor groove. Proc. Natl. Acad. Sci. USA **89**:11779–11783.
8. **Gartenberg, M. R., C. Ampe, T. A. Steitz, and D. M. Crothers.** 1990. Molecular characterization of the GCN4-DNA complex. Proc. Natl. Acad. Sci. USA **87**:6034–6038.
9. **Hai, T., and T. Curran.** 1991. Fos/Jun and ATF/CREB cross-family dimerization alters DNA binding specificity. Proc. Natl. Acad. Sci. USA **88**:3720–3724.
10. **Hai, T., F. Liu, W. J. Coukos, and M. R. Green.** 1989. Transcription factor ATF cDNA clones: an extensive family of leucine zipper proteins able to selectively for DNA binding heterodimers. Genes Dev. **3**:2083–2090.
11. **Hoeffler, J. P., J. W. Lustbader, and C.-Y. Chen.** 1991. Identification of multiple nuclear factors that interact with cyclic adenosine 3′,5′-monophosphate response element-binding protein and activating transcription factor-2 by protein-protein interactions. Mol. Endocrinol. **5**:256–266.
12. **Jain, J., P. G. McCaffrey, Z. Miner, T. Kerppola, J. N. Lambert, G. L. Verdine, T. Curran, and A. Rao.** The T cell transcription factor NFATp is a substrate for calcineurin and interacts with the DNA-binding domains of Fos and Jun. Nature (London), in press.
13. **Kerppola, T. K., and T. Curran.** 1991. Transcription factor interactions: basics on zippers. Curr. Opin. Struct. Biol. **1**:71–79.
14. **Kerppola, T. K., and T. Curran.** 1991. Fos-Jun heterodimers and Jun homodimers bend DNA in opposite orientations: implications for transcription factor cooperativity. Cell **66**:317–326.
15. **Kerppola, T. K., and T. Curran.** 1991. DNA bending by Fos and Jun: the flexible hinge model. Science **254**:1210–1214.
16. **Kerppola, T. K., and T. Curran.** 1993. DNA bending by Fos and Jun: structural and functional implications, p. 70–105. *In* F. Eckstein and D. M. Lilley (ed.), Nucleic acids & molecular biology, vol. 7. Springer-Verlag, Berlin.

16a. **Kerppola, T. K., and T. Curran.** Unpublished data.

17. **Kerppola, T. K., D. Luk, and T. Curran.** 1993. Fos is a preferential target of glucocorticoid receptor inhibition of AP-1 activity in vitro. Mol. Cell. Biol. **13**:3782–3791.
18. **Li, L., J. Chambard, M. Karin, and E. N. Olson.** 1992. Fos and Jun repress transcriptional activation by myogenin and MyoD: the amino terminus of Jun can mediate repression. Genes Dev. **6**:676–689.
19. **Lieberman, P. M., and A. J. Berk.** 1991. The Zta *trans*-activator protein stabilizes TFIID association with promoter DNA by direct protein-protein interaction. Genes Dev. **5**:2441–2454.
20. **Maekawa, T., H. Sakura, C. Kanei-Ishii, T. Sudo, T. Yoshimura, J. Fujisawa, M. Yoshida, and R. Ishii.** 1989. Leucine zipper structure of the protein CRE-BP1 binding to the cAMP response element in brain. EMBO J. **8**:2023–2028.
21. **Nishina, H., N. Sato, T. Suzuki, M. Sato, and H. Iba.** 1990. Isolation and characterization of *fra-2*, an additional member of the *fos* gene family. Proc. Natl. Acad. Sci. USA **87**:3619–3623.
22. **O'Shea, E. K., J. D. Klemm, P. S. Kim, and T. Alber.** 1991. X-ray structure of the GCN4 leucine zipper, a two-stranded, parallel coiled coil. Science **254**:539–544.
23. **Ryder, K., S. Silver, A. L. DeLucia, E. Fanning, and P. Tegtmeyer.** 1986. An altered DNA conformation in origin region I is a determinant for the binding of SV40 large T antigen. Cell **44**:719–725.
24. **Ryseck, R.-P., and R. Bravo.** 1991. c-Jun, Jun B, and Jun D differ in their binding affinities to AP-1 and CRE consensus sequences: effect of Fos proteins. Oncogene **6**:533–542.
25. **Schüle, R., K. Umesono, D. J. Mangelsdorf, J. Bolado, J. W. Pike, and R. M. Evans.** 1990. Jun-Fos and receptors for vitamins A and D recognize a common response element in the human osteocalcin gene. Cell **61**:497–504.

25a. **Sonnenberg, J.** Personal communication.

26. **Spana, C., and V. G. Corces.** 1990. DNA bending is a determinant of binding specificity for a *Drosophila* zinc finger protein. Genes Dev. **4**:1505–1515.
27. **Taylor, I. C. A., J. L. Workman, T. J. Schuetz, and R. E. Kingston.** 1991. Facilitated binding of GAL4 and heat shock factor to nucleosomal templates: differential function of DNA-binding domains. Genes Dev. **5**:1285–1298.
28. **Thompson, J. F., and A. Landy.** 1988. Empirical estimation of protein-induced DNA bending angles: applications to λ site-specific recombination complexes. Nucleic Acids Res. **16**:9687–9705.
29. **Ullman, K. S., J. P. Northrop, A. Admon, and G. R. Crabtree.** 1993. Jun family members are controlled by a calcium-regulated, cyclosporin A-sensitive signaling pathway in activated T lymphocytes. Genes Dev. **7**:188–196.
30. **Verrijzer, C. P., J. A. van Oosterhout, W. W. van Weperen, and P. C. van der Vliet.** 1991. POU proteins bend DNA via the POU-specific domain. EMBO J. **10**:3007–3014.
31. **Wechsler, D. S., and C. V. Dang.** 1992. Opposite orientations of DNA bending by c-Myc and Max. Proc. Natl. Acad. Sci. USA **89**:7635–7639.
32. **Zinkel, S. S., and D. M. Crothers.** 1987. DNA bend direction by phase sensitive detection. Nature (London) **328**:178–181.